Transactions on Modelling and Simulation vol 12, © 1996 WIT Press, www.witpress.com, ISSN 1743-355X

Influence of shear and elongation on drop deformation in a convergent/divergent tube

R.E. Khayat, A. Luciani, L.A. Utracki
National Research Council of Canada,
Industrial Materials Institute,
75 de Mortagne blvd., Boucherville, Quebec, Canada J4B 6Y4

Abstract

We examine the influence of shear and elongation on the planar deformation of a drop as it is driven by the ambient flow of a surrounding fluid flowing in a convergent/divergent tube. A boundary element approach is adopted that requires the solution of two simultaneous integral equations on the drop/fluid interface and tube wall. Effects of the viscosity ratio, the initial position of the drop (with respect to the tube axis) and its diameter (relative to the tube dimension), on the motion of the drop are examined.

1 Introduction

While extensive work has been devoted to the modeling and simulation of drops deforming in an infinite fluid medium, relatively little has been done in the case of a drop deforming in a confined medium. In both cases, most simulations were carried out using the boundary-element method (BEM). Applications of the BEM have ranged from the classical study of a rising drop in an otherwise quiescent fluid,[1,2] to more complex situations such as drop breakup and coalescence,[3] the deformation of biological cells,[4] and the deformation of small drops in electric and magnetic fields.[5] Some studies also included the influence of non-uniform flow such as the deformation of drops in shear flow[6] and extensional flow.[7] More recently, the BEM has been extended to include the motion of a drop in the vicinity of a plane wall,[8] a deformable interface,[9] the deformation of drops in confined flows such as inside a circular tube,[10] or in a tube with

constriction.[11] These latter studies, however, examined only axisymmetric motion; the drop deformation was therefore confined along the axis of the tube.

This paper, is one in the series of publications that explore the applicability of the BEM to problems in materials processing.[12-14] Thus, we examine the influence of shear and elongation on the planar motion of the drop as it deforms inside the tube. This problem is of great importance for the compounding and mixing of polymer blends, where drops of one viscoelastic liquid must be dispersed within another polymer matrix.[15,16] A shear- or elongation-dominated drop deformation will depend on the initial position of the deforming drop with respect to the tube axis and its size relative to the tube dimension(s).

2 Boundary element formulation

Both drop and suspending fluid are assumed to be viscous Newtonian and incompressible. We are particularly interested in low Reynolds number flows that are typically characterized by small velocities, small length scales and/or high fluid viscosities. This assumption is reasonably justified in the present case since the fluids of interest are typical polymers of high viscosity undergoing small strain rates during the flow. In this limit the inertia terms in the Navier-Stokes equations are neglected so the system drop/fluid is in a state of creeping motion. At any instant t, the drop occupies a region $\Omega_d(t)$ and is assumed to be neutrally buoyant so the effects of gravity and any external body forces are neglected. The suspending fluid, which occupies the region $\Omega_s(t)$, is driven by an imposed pressure gradient and flows at a constant volume rate. We assume that the regions $\Omega_d(t)$ and $\Omega_s(t)$ are separated at any time by the moving interface $\Gamma_i(t)$ between drop and the suspending fluid. We thus exclude situations where the drop comes in contact with the tube walls or the drop being too close to the entrance or exit. The region $\Omega_s(t)$ is thus assumed bounded by $\Gamma_i(t)$ and the inner boundary of the tube, $\Gamma_t = \Gamma_{en} \cup \Gamma_{ex} \cup \Gamma_w$, is composed of the inner walls of the tube Γ_w as well as the entrance and exit regions Γ_{en} and Γ_{ex}, respectively. The conservation of mass and linear momentum equations are given for a general flow in region $\Omega(t)$ by:

$$\nabla \cdot \mathbf{u} = 0, \qquad \nabla \cdot \boldsymbol{\sigma} = 0, \qquad \boldsymbol{\sigma} = -p\mathbf{I} + \mu(\nabla \mathbf{u} + \nabla \mathbf{u}^t), \qquad \mathbf{x} \in \Omega(t), \quad (1)$$

where ∇ is the gradient operator, $\mathbf{x}$ the position vector, $\mathbf{u}$ the velocity vector, $\boldsymbol{\sigma}$ the stress tensor, p is the hydrostatic pressure, μ the viscosity of the fluid medium and $\mathbf{I}$ the unit tensor. It is important to note that the acceleration term $\partial \mathbf{u}/\partial t$ in the momentum conservation equation has been neglected, so the formulation in question is quasi-steady. The quasi-steady state assumption is valid whenever $L^2/\nu << \tau$, where L and τ are typical characteristic length and time of flow, and $\nu = \mu/\rho$ is the kinematic

viscosity (ρ being the density). In the present case, since there is no driving velocity in the problem, $\tau \sim L(\rho/\Delta P)^{1/2}$, ΔP being a typical value of the driving pressure. Thus, for the quasi-steady state assumption to apply, one must have $\Delta PL^2/\rho v^2 << 1$. This is indeed typically the case for a polymeric fluid. Note also that this inequality is implied by the smallness of the Reynolds number. Physically, the quasi-steady state approximation means that the fluid immediately adjusts to changes in the location of the interface. Equation (1) must be supplemented by appropriate boundary conditions.

While the boundary conditions at the solid wall are straightforward, those at the interface must be examined more closely. The suspending fluid is assumed to adhere to the solid boundary, so that stick boundary conditions apply on Γ_w. Thus, the flow field is determined through eqn (1) for $\Omega_s(t)$ subject to stick and no penetration at the tube wall Γ_w, dynamic conditions and an appropriately chosen kinematic condition at the interface $\Gamma_i(t)$. The proper choice and implementation of a kinematic condition are not obvious.[17] In a Lagrangian representation, the interface is assumed to deform with the fluid velocity. This procedure tends to sweep points on the surface along the tangent to the surface even if small shape changes actually occur. Consequently, frequent redistribution of surface points becomes necessary. In this paper, the interface is assumed to deform point-wise along the normal with the normal projection of the fluid velocity at the surface.[1] This method has the advantage of keeping the points on the surface evenly distributed. The following kinematic boundary conditions are assumed to hold on $\Gamma_i(t)$:

$$\frac{\mathbf{dx}}{\mathbf{d}t} = \mathbf{n}(\mathbf{x},t)[\mathbf{n}(\mathbf{x},t)\cdot\mathbf{u}(\mathbf{x},t)], \qquad \mathbf{x}\in\Gamma_i(t) \quad (2)$$

where $\mathbf{n}$ is the normal unit vector at the interface directed from the suspending fluid region to the region occupied by the drop. The dynamic conditions on the interface is based on the continuity of the tangential stress (no traction) and discontinuity of normal stress due to interfacial tension:

$$[\sigma_s(\mathbf{x},t)-\sigma_d(\mathbf{x},t)]\cdot\mathbf{n}(\mathbf{x},t) = \gamma\mathbf{n}(\mathbf{x},t)\nabla\cdot\mathbf{n}(\mathbf{x},t), \qquad \mathbf{x}\in\Gamma_i(t) \quad (3)$$

where γ is the relative interfacial tension. Subscripts s and d are used to refer to flow variables in the suspended fluid and drop regions, respectively. Note that eqn (3) was derived assuming equilibrium conditions and uniform surface tension under dynamic conditions.[18] The continuity of velocity also applies at the interface:

$$\mathbf{u}_s(\mathbf{x},t)-\mathbf{u}_d(\mathbf{x},t) = 0, \qquad \mathbf{x}\in\Gamma_i(t). \quad (4)$$

The integral representation of the Stokes equations in the two fluid regions $\Omega_S(t)$ and $\Omega_d(t)$ is based on the Reciprocal (Green's) Theorem, which relates the fields $(\mathbf{u}, \sigma)$ to the fundamental solution $(\mathbf{u}^*, \sigma^*)$.[16] We denote by λ the drop-to-fluid viscosity ratio, while the velocity and traction by $\mathbf{u}_d(\mathbf{x},t)$ and $\mathbf{t}_d(\mathbf{x},t)$ in the drop region $\Omega_d(t)$, and by $\mathbf{u}_S(\mathbf{x},t)$ and $\mathbf{t}_S(\mathbf{x},t)$ in the suspending fluid region $\Omega_S(t)$, obtaining the following integral equations:

$$\int_{\Gamma_t \cup \Gamma_i(t)} \left[\frac{1}{\mu} \mathbf{t}_S(\mathbf{y},t) \cdot \mathbf{J}(\mathbf{x}|\mathbf{y}) - \mathbf{u}_S(\mathbf{y},t) \cdot \mathbf{K}(\mathbf{x}|\mathbf{y}) \right] d\Gamma(\mathbf{y}) = \begin{cases} \mathbf{u}_S(\mathbf{x},t) & \mathbf{x} \in \Omega_S \\ \dfrac{\mathbf{u}_S(\mathbf{x},t)}{2} & \mathbf{x} \in \Gamma_t \cup \Gamma_i \\ \mathbf{0} & \mathbf{x} \in \Omega_d \end{cases}$$

(5)

$$\int_{\Gamma_i(t)} \left[\mathbf{u}_d(\mathbf{y},t) \cdot \mathbf{K}(\mathbf{x}|\mathbf{y}) - \frac{1}{\mu\lambda} \mathbf{t}_d(\mathbf{y},t) \cdot \mathbf{J}(\mathbf{x}|\mathbf{y}) \right] d\Gamma(\mathbf{y}) = \begin{cases} \mathbf{0} & \mathbf{x} \in \Omega_S \cup \Gamma_t \\ \dfrac{1}{2}\mathbf{u}_d(\mathbf{x},t) & \mathbf{x} \in \Gamma_i \\ \mathbf{u}_d(\mathbf{x},t) & \mathbf{x} \in \Omega_d \end{cases}$$

Note that $\mathbf{J}$ and $\mathbf{K}$ are second and third rank tensors, respectively, given by:

$$\mathbf{J}(\mathbf{x}|\mathbf{y}) = \frac{1}{4\pi}\left(\mathbf{I}\log r - \frac{\mathbf{rr}}{r^2} \right), \qquad \mathbf{K}(\mathbf{x}|\mathbf{y}) = -\frac{1}{\pi}\frac{\mathbf{rrr}}{r^4}, \tag{6}$$

for an unbounded two-dimensional domain. Here $\mathbf{r} = \mathbf{x} - \mathbf{y}$ is the relative position between the field point and source point, and $r = |\mathbf{r}|$. We are particularly interested in the evolution of the interface; the variable of main interest is thus the velocity at the interface $\mathbf{u}_d(\mathbf{x} \in \Gamma_i,t) = \mathbf{u}_S(\mathbf{x} \in \Gamma_i,t)$. Note that the tractions on each side of the interface must also be determined. We can, however, take advantage of condition (3) that relates the normal tractions in terms of the interfacial tension, and eliminate the tractions at the interface altogether. For this, we multiplying the first of eqn (5) by λ, adding to the second equation, and using the boundary conditions (3) and (4) to yield:

$$\int_{\Gamma_t}\left[\mathbf{u}_s(\mathbf{y},t)\cdot\mathbf{K}(\mathbf{x}|\mathbf{y})-\frac{1}{\mu}\mathbf{t}_s(\mathbf{y},t)\cdot\mathbf{J}(\mathbf{x}|\mathbf{y})\right]d\Gamma(\mathbf{y})+(1-\lambda)\int_{\Gamma_i(t)}\mathbf{u}_d(\mathbf{y},t)\cdot\mathbf{K}(\mathbf{x}|\mathbf{y})d\Gamma(\mathbf{y})$$

$$-\frac{\gamma}{\mu}\int_{\Gamma_i(t)}\left[\nabla_y\cdot\mathbf{n}(\mathbf{y})\right]\mathbf{n}(\mathbf{y})\cdot\mathbf{J}(\mathbf{x}|\mathbf{y})d\Gamma(\mathbf{y})=\begin{cases}\mathbf{u}_s(\mathbf{x},t) & \mathbf{x}\in\Omega_s(t)\\ \left(\frac{\lambda+1}{2}\right)\mathbf{u}_d(\mathbf{x},t) & \mathbf{x}\in\Gamma_i(t)\\ \lambda\mathbf{u}_d(\mathbf{x},t) & \mathbf{x}\in\Omega_d(t)\end{cases}\qquad(7)$$

We also need an integral equation that governs the value of the velocity and traction on the walls of the tube, that can be similarly obtained:

$$\int_{\Gamma_i(t)}\left\{(1-\lambda)\mathbf{u}_d(\mathbf{y},t)\cdot\mathbf{K}(\mathbf{x}|\mathbf{y})-\frac{\gamma}{\mu}\left[\nabla_y\cdot\mathbf{n}(\mathbf{y})\right]\mathbf{n}(\mathbf{y})\cdot\mathbf{J}(\mathbf{x}|\mathbf{y})\right\}d\Gamma(\mathbf{y})+$$

$$\int_{\Gamma_t}\left[\mathbf{u}_s(\mathbf{y},t)\cdot\mathbf{K}(\mathbf{x}|\mathbf{y})-\frac{1}{\mu}\mathbf{t}_s(\mathbf{y},t)\cdot\mathbf{J}(\mathbf{x}|\mathbf{y})\right]d\Gamma(\mathbf{y})=\frac{1}{2}\mathbf{u}_s(\mathbf{x},t)\qquad\mathbf{x}\in\Gamma_t\qquad(8)$$

If the velocity on Γ_t is fully prescribed (as in the present study), then only the traction (in the second integral of the equation above) is determined. Equations (7) and (8) represent coupled equations for the velocity at the interface $\mathbf{u}_d(\mathbf{x}\in\Gamma_i,t)$ and the traction at the walls of the tube $\mathbf{t}_s(\mathbf{x}\in\Gamma_t,t)$. Also, following the determination of these unknowns, the flow field off the interface and tube walls can be calculated using the first and third equations in (7) in the drop region $\Omega_d(t)$ and the region $\Omega_s(t)$ occupied by the suspending fluid. We now turn to the numerical solution of eqns (7) and (8).

The integrals in eqns (7) and (8) are discretized into a finite sum of contributing terms over the boundaries. In this study, we adopt the simplest form of the BEM, and consider the velocity and traction to be constant over each boundary element. We focus the attention on the value of the flow variables on the boundary, assuming that the interface $\Gamma_i(t)$ is subdivided into N_i segments $\Delta\Gamma_i^n$ and the tube wall Γ_t into N_t segments $\Delta\Gamma_t^n$. The number of segments at the interface may vary in time if re-meshing is needed. At each time step of the process, the shape of the interface is determined from the velocity value and shape obtained at the previous time step. There are exactly $2(N_i + N_t)$ unknowns at any time step. The resulting system of linear algebraic equations may be written in the form $\mathbf{HU} = \mathbf{GT} + \mathbf{B}$, where $\mathbf{H}$ and $\mathbf{G}$ are the matrix coefficients of the system and $\mathbf{U}$ and $\mathbf{T}$ are vectors containing the unknown velocity and

traction variables. The matrice coefficients in the system are given as follows:

$$\mathbf{H}_{mn}(t)=\begin{cases}\dfrac{1}{2}\delta_{mn}+\displaystyle\int_{\Delta\Gamma_t^n}\mathbf{K}(\mathbf{x}_m,\mathbf{y})d\Gamma(\mathbf{y}), & m\in[1,N_t+N_i],\ n\in[1,N_t]\\ \dfrac{\lambda+1}{2}\delta_{mn}+\displaystyle\int_{\Delta\Gamma_i^n}\mathbf{K}(\mathbf{x}_m,\mathbf{y})d\Gamma(\mathbf{y}) & m\in[1,N_t+N_i],\ n\in[N_t+1,N_t+N_i]\end{cases}$$

$$\mathbf{G}_{mn}=\begin{cases}\dfrac{1}{\mu}\displaystyle\int_{\Delta\Gamma_t^n}\mathbf{J}(\mathbf{x}_m,\mathbf{y})d\Gamma(\mathbf{y}), & m\in[1,N_t+N_i],\ n\in[1,N_t]\\ 0 & m\in[1,N_t+N_i],\ n\in[N_t+1,N_t+N_t]\end{cases}$$

$$\mathbf{B}_{mn}(t)=\begin{cases}0 & m\in[1,N_t+N_i],\ n\in[1,N_t]\\ \dfrac{\gamma}{\mu}\kappa^n(t)\mathbf{n}^n(t)\cdot\displaystyle\int_{\Delta\Gamma_i^n}\mathbf{J}(\mathbf{x}_m,\mathbf{y})d\Gamma(\mathbf{y}), & m\in[1,N_t+N_i],\ n\in[N_t+1,N_t+N_t]\end{cases}$$

where $\mathbf{x}_m$ is the position vector of the center of the segment. Note that coefficients H_{mn} and B_{mn} are time dependent while G_{mn} are constant. The algebraic system above is solved using the LU factorization method. The inner flow field in the drop and suspending fluid regions may then be determined from the first and third equations of (7) once the unknown variables are determined on the boundary.

3 Numerical results

In this section, we examine the planar deformation of droplets subjected to the flow field of the suspending fluid, inside a parabolic convergent/divergent tube (Figure 1). We are particularly interested in the influence of ambient shear and elongation on the drop deformation. Several influencing parameters may be examined in this case; we focus our attention on the effects of viscosity ratio and initial drop position relative to the tube axis. We assume that at time $t = 0$, the drop is suddenly placed near the entrance region of the tube, and is subsequently subject to the motion of the suspending fluid. Strictly speaking, the quasi steady-state hypothesis assumed in the formulation is not valid since the drop is practically subjected to a sudden motion (acceleration) at $t > 0$. The size of the drop and its initial position relative to the axis of the tube are determining factors on the drop deformation as to the dominance of either shear or elongation effect from the suspending fluid. Thus, if the drop is large relative to the tube opening, or positioned far from the tube axis, then

the influence of shear flow from the boundary layer in the vicinity of the tube wall becomes significant. On the other hand, if the drop size is relatively small, or the drop is moving close to the tube axis, then the flow elongation is most influential. The effect of the interfacial energy was neglected in the following results.

We first examine the influence of the viscosity ratio in the range $\lambda \in [0.5, 5]$ for a drop of initial radius of 4 mm deforming along the tube axis. The resulting deformation for the various viscosity ratios are shown in Figure 2. For the situations corresponding to the higher viscosity ratios, the drop tends to deform more like a solid as it resists deformation. The drops were observed to elongate when approaching the neck region of the tube, where most of the elongational flow is concentrated along the axis and stretching the drop by more than twice its initial diameter. The influence of shear flow becomes mostly visible as the drop exits from the neck region, with its tail starting to deform leading to the formation of two tails. It is interesting to observe that for $\lambda > 2$, the shape of the drop as it approaches the exit region is independent of viscosity ratio.

The situation is quite different when the drop viscosity is smaller than that of the suspending fluid ($\lambda = 0.5$). In this case, the drop is observed to deform significantly as it approaches the neck region. The deformation is clearly symmetric as the drop recovers its circular shape at the exit of the neck region. This shape recovery is most likely not due to the small viscosity ratio but results rather from the high stretching deformation that the drop undergoes in the neck region where elongation tends to dominate over shear flow. In contrast to the cases with $\lambda > 2$, the drop diameter has decreased significantly in the neck region for any shear influence to be significant on the subsequent deformation. The evolution of the deformation with respect to the position is also shown in Figure 3 for various viscosity ratios. The figure confirms the general tendency of the drop deformation to increase and reach a maximum as the drop enters the neck region, to then decrease as it nears the exit of the tube. The figure also shows that the maximum tends to shift away from the middle of the tube as the viscosity ratio increases.

In order to further assess the interplay between shear and elongation, we examine the influence of the initial position of the drop. We have placed a drop (of relative viscosity $\lambda = 2$) off the axis, and the subsequent deformation is shown in Figure 4 in comparison to that of a drop initially positioned on the axis. The deformation of the latter is similar to that shown in Figure 2 although the drop is twice smaller. The drop, located initially off the axis, is observed to stretch more in the converging region of the tube than the one placed on the axis. It tends to be dragged (relatively) away from the tube wall into the center along the tube axis, and then swept back into the region near the wall as it exits the neck region. At this point, the drop remains significantly stretched and does not recover its circular shape as the drop located along the axis tends to do.

We also examined the influence of drop position relative to the tube axis for two additional viscosity ratios as shown in Figures 5 and 6 for λ = 0.9 and 10, respectively. The two figures show clearly the increase in deformation as the drop is initially placed farther from the axis. Figure 5 indicates that the maximum deformation tends to occur at a position further away from the neck region and towards the exit zone as the drop is initially farther from the axis. For a relatively high viscosity ratio, Figure 6 indicates, unexpectedly, the presence of relatively significant deformation for the drop initially positioned farthest from the tube axis; this deformation is due to pronounced shearing, and would be essentially absent for purely elongational flow.

4 Conclusion

The influence of shear and elongation is examined on the deformation of a Newtonian drop as it is suspended in an ambient fluid flowing inside a convergent/divergent tube. It is found that a small drop, placed initially on the tube axis, tends to recover its initial shape in the divergent zone, whereas a drop that is initially closer to the tube wall tends to stretch indefinitely. A large drop with a relatively small viscosity also tends to recover its initial shape because of the high degree of elongation that the drop undergoes in the neck region. Thus, shearing may deform significantly a drop as opposed to elongation which tends to help the drop recover its circular shape. It is also found that relatively large deformation can occur for a drop of relatively large viscosity (λ = 10) which, in a purely elongational flow, would not have deformed significantly (see Figure 6).

1. Koh, C.J. & Leal, L G. The stability of drop shapes for translation at zero Reynolds number through a quiescent fluid, *Phys. Fluids* A, 1989, **1**, 1309.

2. Pozrikidis, C. The instability of a moving viscous drop, *J. Fluid Mech.*, 1990, **210**, 1.

3. Li, X.Z. Barthes-Bielsel, D. & Helmy, A. Large deformations and burst of a capsule freely suspended in an elongational flow, *J. Fluid Mech.*, 1988, **187**, 179.

4. Zinemanas, D. & Nir, A. On the viscous deformation of biological cells under anisotropic surface tension, *J. Fluid Mech.*, 1988, **217**, 217.

5. Sherwood, J.D. Breakup of fluid droplets in electric and magnetic fields, *J. Fluid Mech.*, 1988, **188**, 133.

6. Rallison, J.M. The deformation of small viscous drops and bubbles in shear flows, *Ann. Rev. Fluid Mech.*, 1984, **16**, 45.

7. Rallison, J.M. & Acrivos, A. A numerical study of the deformation and burst of a viscous drop in an extensional flow, *J. Fluid Mech.*, 1978, **89**, 191.

8. Ascoli, E.P., Dandy, D.S. & Leal, L.G. Boundary-driven motion of a deformable drop toward a planar wall at low Reynolds number, *J. Fluid Mech.*, 1990, **213**, 287.

9. Yiantsios, S.G. & Davis, R.H. On the buoyancy-driven motion of a drop towards a rigid or deformable interface, *J. Fluid Mech.*, 1990, **217**, 547.

10. Martinez, M.J. & Udell, K.S. Axisymmetric creeping motion of drops through circular tubes, *J. Fluid Mech.*, 1990, **210**, 565.

11. T.M. Tsai and M.J. Miksis, Dynamics of a drop in a constricted capillary tube, *J. Fluid Mech.* **274** (1994) 197.

12. Khayat, R.E., Derdouri, A. & Hebert, L.P. A boundary-element approach to three-dimensional gas-assisted injection molding, *J. Non-Newt. Fluid Mech.*, 1995, **57**, 253.

13. Frayce, D. & Khayat, R.E. A dual reciprocity boundary element approach to three-dimensional transient heat conduction as applied to materials processing, *Num. Heat Transfer* A, 1996, **29**, 243.

14. Khayat, R.E., Derdouri, A. & Frayce, D. On the application of the boundary-element method to three-dimensional transient mixing processes, *J. Non-Newt. Fluid Mech.* (in press).

15. Utracki, L.A., & Luciani, A. Mixing in extensional flow field, *Intl. Plast. Eng. Technol.*, 1996, **2**, 000.

16. Luciani, A., & Utracki, L.A. The extensional flow mixer, EFM, *Intl. Polymer Process.* (in press).

17. Floryan, J.M. & Rasmussen, H. Numerical methods for viscous flows with moving boundaries, *App. Mech. Rev.*, 1989, **42**, 323.

18. Batchelor, G.K. *Introduction to Fluid Dynamics,* Cambridge University Press, 1967.

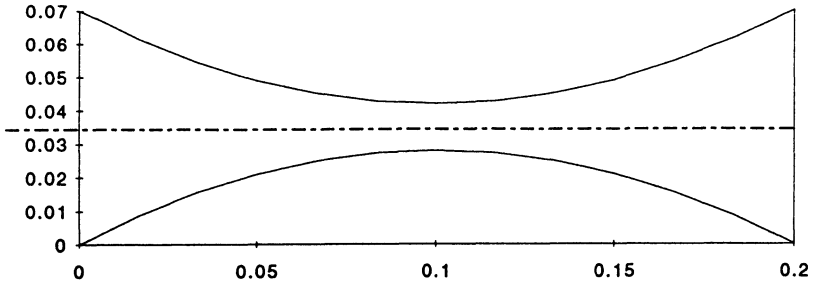

Figure 1. Convergent/divergent tube geometry and dimensions (m)

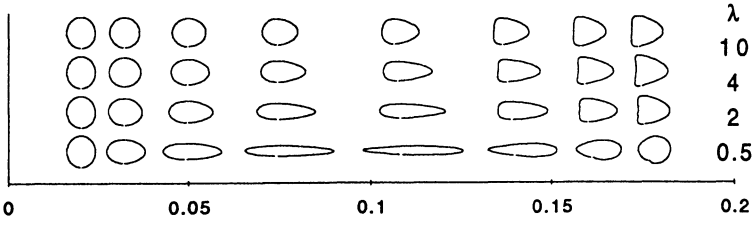

Figure 2. Effect of viscosity ration λ on deformation along tube axis

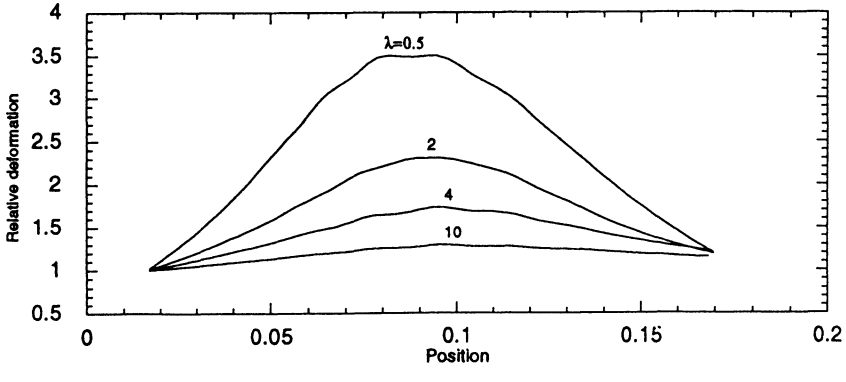

Figure 3. Relative deformation along tube axis as function of λ

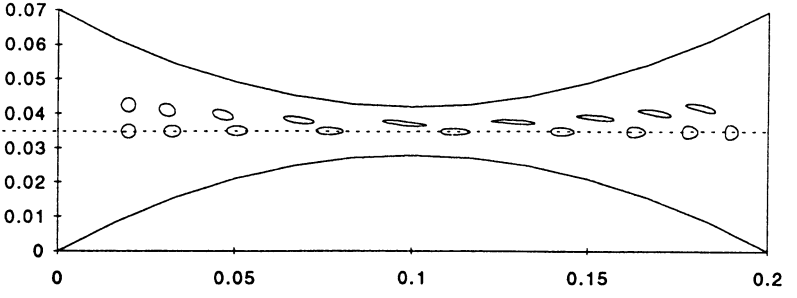

Figure 4. Effect of initial position on relative deformation ($\lambda = 2$).

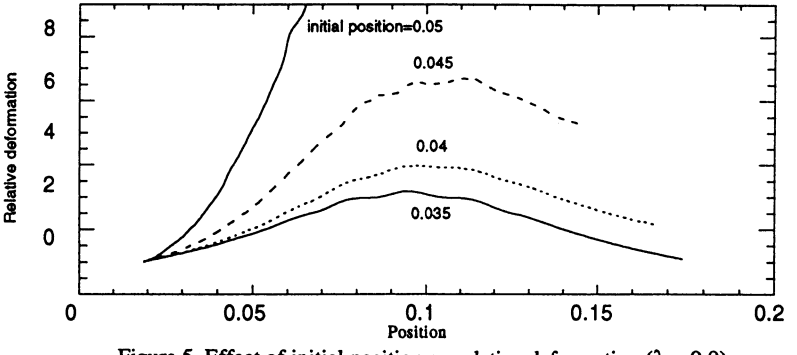

Figure 5. Effect of initial position on relative deformation ($\lambda = 0.9$).

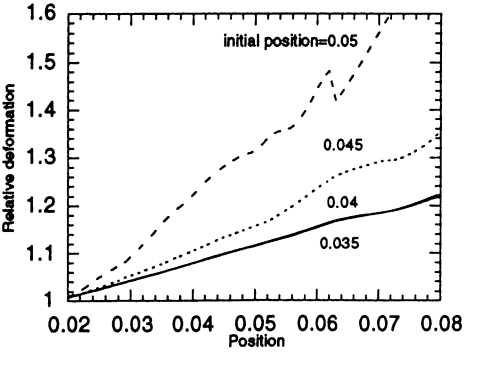

Figure 6. Effect of initial position on relative deformation ($\lambda = 10$).